

# Effects of Residual Stress on Fracture Strength of Si<sub>3</sub>N<sub>4</sub>/Stainless Steel Joints With a Cu-Interlayer

Hwisouck Chang, Sang-Whan Park, Sung-Churl Choi, and Tae-Woo Kim

(Submitted 26 June 2002)

The variation in fracture strength of a brazed Si<sub>3</sub>N<sub>4</sub>/Cu/steel joint was compared with the change in residual stress as a function of the Cu-interlayer thickness that was used. The higher residual stress and the lower measured fracture strength for the joint, using a 0.1 mm thick Cu-interlayer, were ascribed to the entire dissolution of the Cu-interlayer into the brazing alloy. The finite element analysis of residual stress, which considered the microstructure at the interface region, could explain the fracture behavior for the brazed joints, which is dependent on the thickness of the Cu-interlayer.

**Keywords** brazing, interlayer, joining, silicon-nitride

## 1. Introduction

The Si-based nonoxide ceramics, including silicon nitride and silicon carbide, have been the object of extensive research and development for structural applications. The commercialization of advanced structural ceramics<sup>[1]</sup> has been practiced with limited success due to their low fracture toughness and high manufacturing cost. The ceramic-to-metal joining technology<sup>[2]</sup> has been adopted to compensate for the brittle nature as well as the high production cost of engineering ceramics, while maintaining the attractive properties of ceramics. The active metal brazing<sup>[2,3]</sup> technique, as processed at an elevated temperature, is known to generate residual stress within the joint due to the mismatch in thermal expansion coefficient (CTE) between mating materials.

Maximum tensile residual stress within ceramic/metal joints is usually developed within a ceramic, because a ceramic tends to have a smaller CTE than a metal.<sup>[2]</sup> Such a residual stress has been known to affect the fracture strength of ceramic/metal joints in inverse proportion. The maximum residual stress developed in the joints could be reduced with the use of an interlayer material in the joint. Previous studies<sup>[4,5]</sup> have shown that the joints with an interlayer exhibiting low yield strength can lower the residual stress through plastic deformation of an interlayer, thus leading to improved fracture strength. Therefore, a good estimation of expected residual stress is important to determine the joint configuration that can exhibit improved ensuing fracture strength.

The Finite Element Analysis (FEA), which is performed on the basis of the given joint geometries, enables the prediction and control of the residual stress in the joint reasonably well. In addition to controlling the residual stress in the neighborhood

of the interface, it is important to ensure chemical compatibility.<sup>[6]</sup> The chemical interactions between joined materials, if not taken into consideration, could cause unexpected compatibility problems during the course of brazing.<sup>[6]</sup> In addition, the overlooked chemical effects are reported to be the primary cause of the disagreement between the measured and the predicted joint properties.<sup>[7]</sup> The qualitative disagreement between measured findings and prediction are considered to stem from the disregarded property changes in the vicinity of the material interface region, where microstructural evolution due to chemical effects takes place.<sup>[8-11]</sup> As CTE-mismatch together with chemical compatibility are primary issues for parts of coating,<sup>[12]</sup> electronic,<sup>[13]</sup> and high-temperature components,<sup>[14]</sup> information about microstructural change induced by interdiffusion is important because they could eventually affect the joint strength.

In the current study, changes in the microstructure of the brazed joints were examined as a function of the used interlayer thickness that was used, and were considered in the finite element modeling stage. The residual stress was then computed on the basis of the changed microstructure for the brazed Si<sub>3</sub>N<sub>4</sub>/stainless steel 316 joint.

## 2. Experimental Procedure

Hipped silicon nitride (Si<sub>3</sub>N<sub>4</sub>) with 6 wt.% of Y<sub>2</sub>O<sub>3</sub> as a sintering additive and stainless steel 316 were used for base materials to be brazed. Pure copper (purity > 99%), with thickness ranging between 0.1-0.8 mm, was used as an interlayer. The filler metal for brazing was Ag-35 wt.% Cu-2 wt.% Ti alloy Cusil-ABA (Wesgo, Inc., Belmont, CA), and its thickness was about 0.05 mm as-received. The relevant thermo-mechanical properties of materials used for the joint are shown in Table 1. All materials used for brazing were washed in ultrasonic cleaner using trichloro-ethylene, acetone, and isopropanol solutions, sequentially. The brazing was performed at a temperature of 850 °C for 10 min under vacuum of about 1.3 MPa. The cooling rate was maintained below 5 °C/min down to 250 °C and then furnace-cooled to room temperature. A Si<sub>3</sub>N<sub>4</sub> block of 3 × 4 × 15 mm in size was bonded to the stainless steel of an identical dimension. The joint strength was evaluated by 4-point bending tests under a crosshead speed of 0.5 mm/min

Hwisouck Chang and Sung-Churl Choi, Department of Inorganic Material Engineering, Hanyang University, Seoul, 133-791, Korea; Sang-Whan Park, Multifunctional Ceramics Research Center, Korea Institute of Science and Technology, Seoul, 136-791, Korea; and Tae-Woo Kim, School of Mechanical Engineering, Kook-Min University, Seoul, 136-702, Korea. Contact e-mail: twkim@kookmin.ac.kr.

with inner and outer spans of 10 and 20 mm, respectively. Scanning electron microscopy (SEM) microstructure in the interfacial region was considered in FEA modeling.

A commercial finite element program, ABAQUS,<sup>[15]</sup> was used to compute the residual stress due to thermal-mismatch, which is developed within the joint during cooling from the brazing temperature. Three-dimensional block elements were adopted, which is based on the geometry of bending test specimen. The fracture surfaces of Si<sub>3</sub>N<sub>4</sub>/stainless steel joints were also examined by using SEM and energy dispersive spectroscopy (EDS).

### 3. Results and Discussion

Figure 1 shows SEM microstructures in the interface region for Si<sub>3</sub>N<sub>4</sub>/stainless steel joints with Cu-interlayers of 0.1 and 0.2 mm in thickness. For Fig.1(a), it was found that the Cu-interlayer of 0.1 mm thickness entirely dissolved into the neighboring brazing alloy, which is interfaced at both sides of the Cu-interlayer. As a result of complete dissolution, the use of a Cu-interlayer of 0.1 mm in thickness leaves virtually no Cu-interlayer. The white and dark regions indicate the silver-

rich and copper-rich regions, respectively. The low-viscosity of the brazing alloy at brazing temperature caused flowing-out. Thus, the brazing alloy, which was originally about 0.05 mm in thickness, was reduced to be about 0.03 mm after brazing.

Examining the interface area revealed that the Cu-interlayer thicker than 0.2 mm also showed a similar amount of dissolution of Cu-interlayer into both sides of the neighboring brazing alloy. The use of the Cu-interlayer of 0.2 mm, which experienced equivalent dissolution of 0.05 mm from both sides of the interface, appeared to retain only about 0.1 mm of the central portion of Cu-interlayer. Consequently, the original thickness for the Cu-interlayer was reduced by 0.1 mm for the entire Cu-interlayer. Only the central portion of Cu-interlayer remained after the brazing process. The dissolution of the Cu-interlayer into the brazing alloy, leading to the composition change in brazing alloy, was also reported for brazed AlN/Cu or ZrO<sub>2</sub>/Cu joints using Cu as an interlayer.<sup>[16,17]</sup>

The dissolution-induced change in microstructure in the interface region is associated with the composition change and is accompanied by the property change in the region. Microhardness is reported to vary in the interface region due to interdiffusion.<sup>[8,9]</sup> The dissolution is expected to decrease the ductility of the brazing alloy, which in turn increases the yield strength of the brazing alloy in the interface area. The increase of the yield strength prevents an efficient relaxation of the residual stress through plastic deformation upon cooling from the brazing temperature.<sup>[4,5]</sup> Furthermore, the dissolution of the Cu-interlayer resulted in a virtual increase in region for the brazing alloy. In the present FEA, a 10% increase in the yield strength was assumed for the brazing alloy region experiencing Cu-dissolution.

The maximum residual stress is reported to be developing near the free edge in the neighborhood of the material interface.<sup>[4,5]</sup> The maximum residual stress developed in Si<sub>3</sub>N<sub>4</sub>, which was predicted by FEA, was plotted as a function of the distance from the interface as shown in Fig. 2. It is important to note that there was a location shift for maximum residual stress depending on the thickness of the Cu-interlayer. For the Si<sub>3</sub>N<sub>4</sub>/stainless steel joint with a 0.1 mm thick Cu-interlayer, the maximum residual stress was found to be developing within

**Table 1 Mechanical Properties for Materials Used in the Joint**

	Young's Modulus, GPa	Poisson's Ratio	Thermal Expansion Coefficient, 10 <sup>-6</sup> /°C	Yield Strength MPa
Si <sub>3</sub> N <sub>4</sub>	300	0.22	3.2	870(a)
Cu	120	0.37	17.7	70
Stainless Steel 316	150	0.25	14.0	240
Cusil ABA (Ag-Cu-Ti)	83	0.36	18.5	271

(a) Fracture strength.

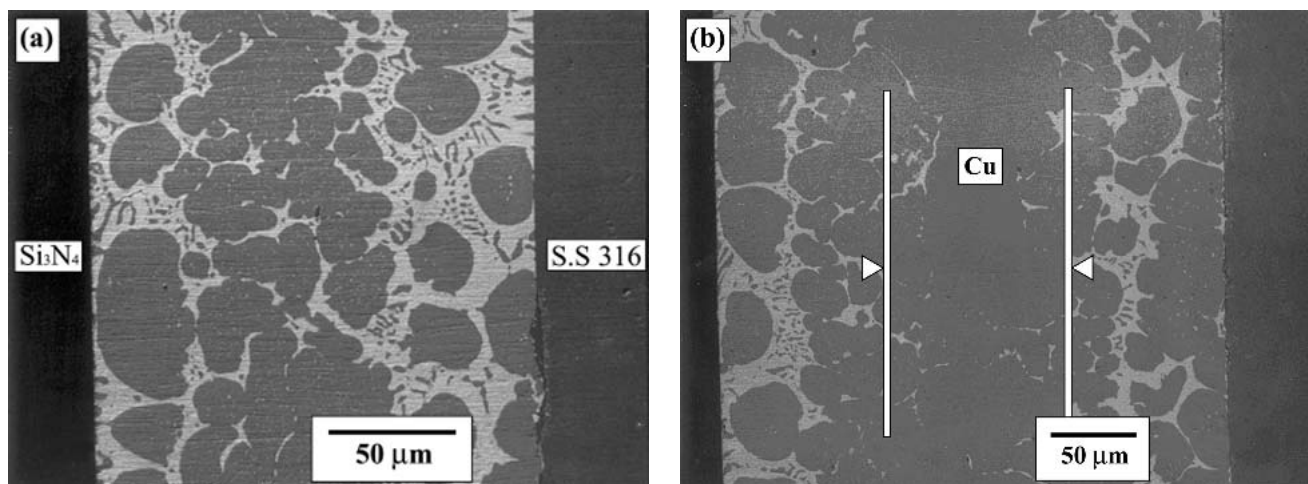


**Fig. 1** SEM microstructure in the interface region of Si<sub>3</sub>N<sub>4</sub>/Cusil ABA/Cu/Cusil ABA/S.S. 316 joint (a) Cu 0.1 mm; (b) Cu 0.2 mm

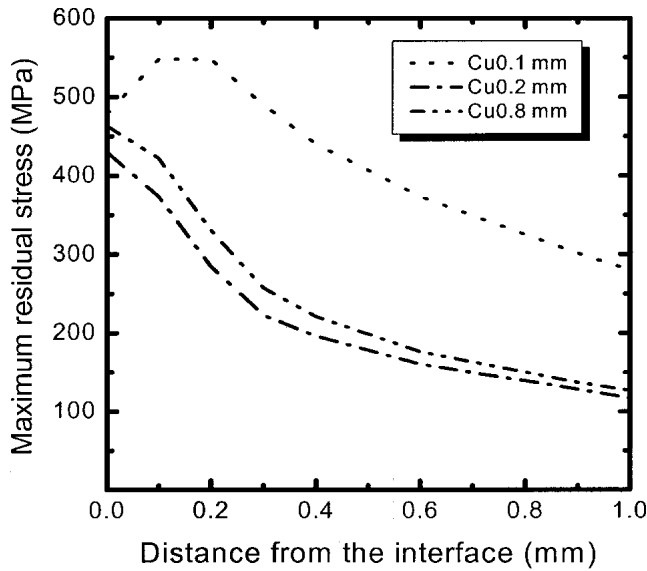


**Fig. 2** Variation of maximum residual stress with distance from the interface for  $\text{Si}_3\text{N}_4/\text{Cu}/\text{S.S. 316}$  joint depending on the thickness of Cu-interlayer

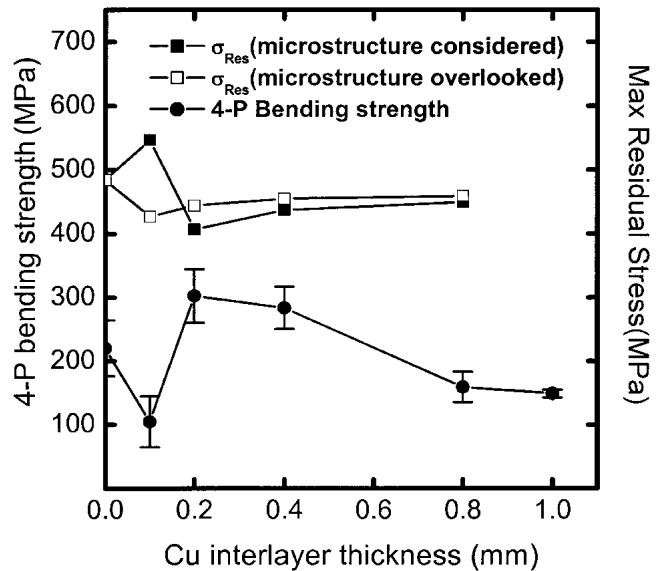


**Fig. 3** Comparison of maximum residual stress and bending strength for  $\text{Si}_3\text{N}_4/\text{Cu}/\text{S.S. 316}$  joint as a function of Cu-interlayer thickness

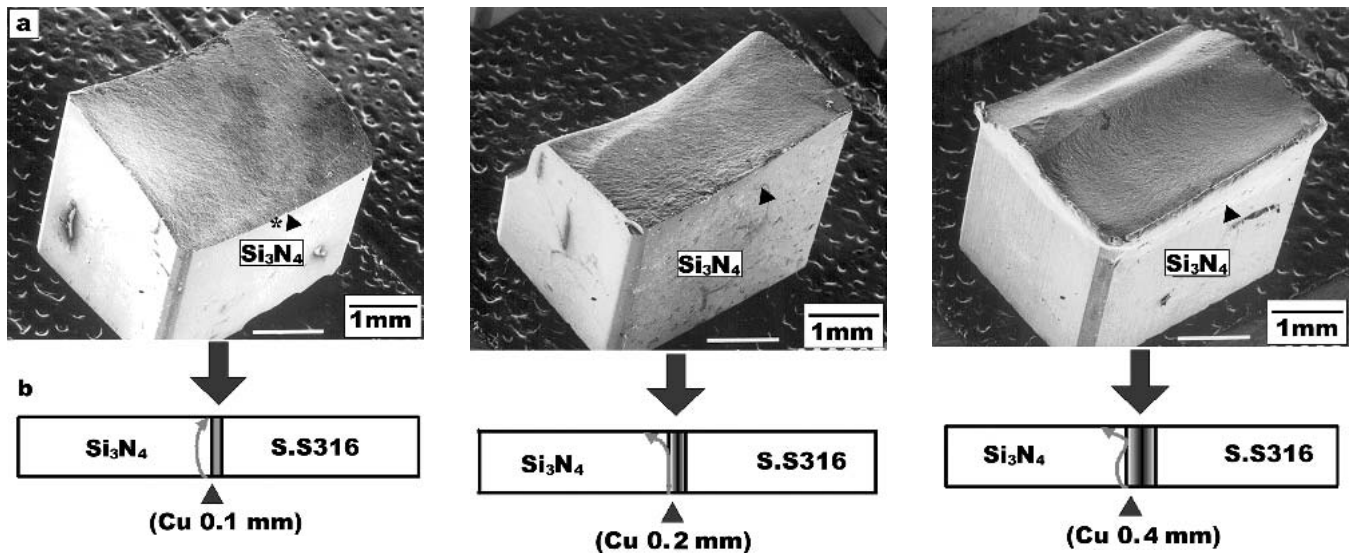


**Fig. 4** Fracture surface of  $\text{Si}_3\text{N}_4/\text{Cu}/\text{S.S.316}$  joint with (a) 3-dimensional SEM views; (b) 2-dimensional schematic views [\* Arrow tip (▲) indicates the specimen side under tensile bend loading]

$\text{Si}_3\text{N}_4$  slightly apart from the interface. Therefore, the fracture for the  $\text{Si}_3\text{N}_4/\text{stainless steel}$  joint with a 0.1 mm thick Cu-interlayer is expected to occur slightly apart from the  $\text{Si}_3\text{N}_4/\text{stainless steel}$  interface region within the bulk of the  $\text{Si}_3\text{N}_4$ . However, the maximum residual stress for the joint with a Cu-interlayer thicker than 0.2 mm invariably occurred at the immediate  $\text{Si}_3\text{N}_4/\text{braze}$  interface. Consequently, the fracture initiation site for the joint with a Cu-interlayer thicker than 0.2 mm is anticipated at the immediate interface.

Figure 3 shows a comparison of the maximum residual stress calculated for  $\text{Si}_3\text{N}_4/\text{stainless steel}$  joints and the measured 4-point bending strength variation depending on the

thickness of the Cu-interlayer. The change in fracture strength (solid circle, ●) appears to represent the inverse variation of the predicted residual stress (solid square, ■) reasonably well. The decreased fracture strength and the increased residual stress for the joint with a Cu-interlayer thicker than 0.1 mm generally shows an inverse nature between the fracture strength and the residual stress within the joint. However, the residual stress computation without considering dissolution-related microstructure change (hollow square, □) does not exhibit an inverse nature between the fracture strength and the residual stress properly. Therefore, it is believed that the microstructure, which is related to interdiffusion at the interface, needs to be

examined and used in the FEA modeling to yield valid comparison between measured findings and predictions.

The largest fracture strength, 310 Mpa, was obtained for the joint with a 0.2 mm thick Cu-interlayer, when the maximum residual stress was predicted to be the lowest among the joints investigated. In spite of the employment of the 0.1 mm thick Cu-interlayer, the entire dissolution of the Cu-interlayer into the brazing alloy has virtually eliminated the presence of the Cu-interlayer as described in Fig. 1. The plastic deformation of a Cu-interlayer appeared to play a role in reducing residual stress starting from a 0.2 mm thick Cu-interlayer, when por-

tions of the Cu-interlayer remained after brazing. Considering that the thermo-elastic properties of stainless steel are similar to those of carbon steel (S45C), it is natural that the extent of the variation in residual stress for  $\text{Si}_3\text{N}_4/\text{Cu}/\text{stainless steel}$  is comparable to that measured for  $\text{Si}_3\text{N}_4/\text{Cu}/\text{carbon-steel}$  employing x-ray.<sup>[18]</sup> Without considering the dissolution of the Cu-interlayer into the brazing alloy during FEA modeling, the onset of decrease in residual stress would have been for the joint with a Cu-interlayer of 0.1 mm in thickness instead of a Cu-interlayer of 0.2 mm as exhibited in Fig. 3. It is regarded, therefore, that the dissolution of the Cu-interlayer into the braz-

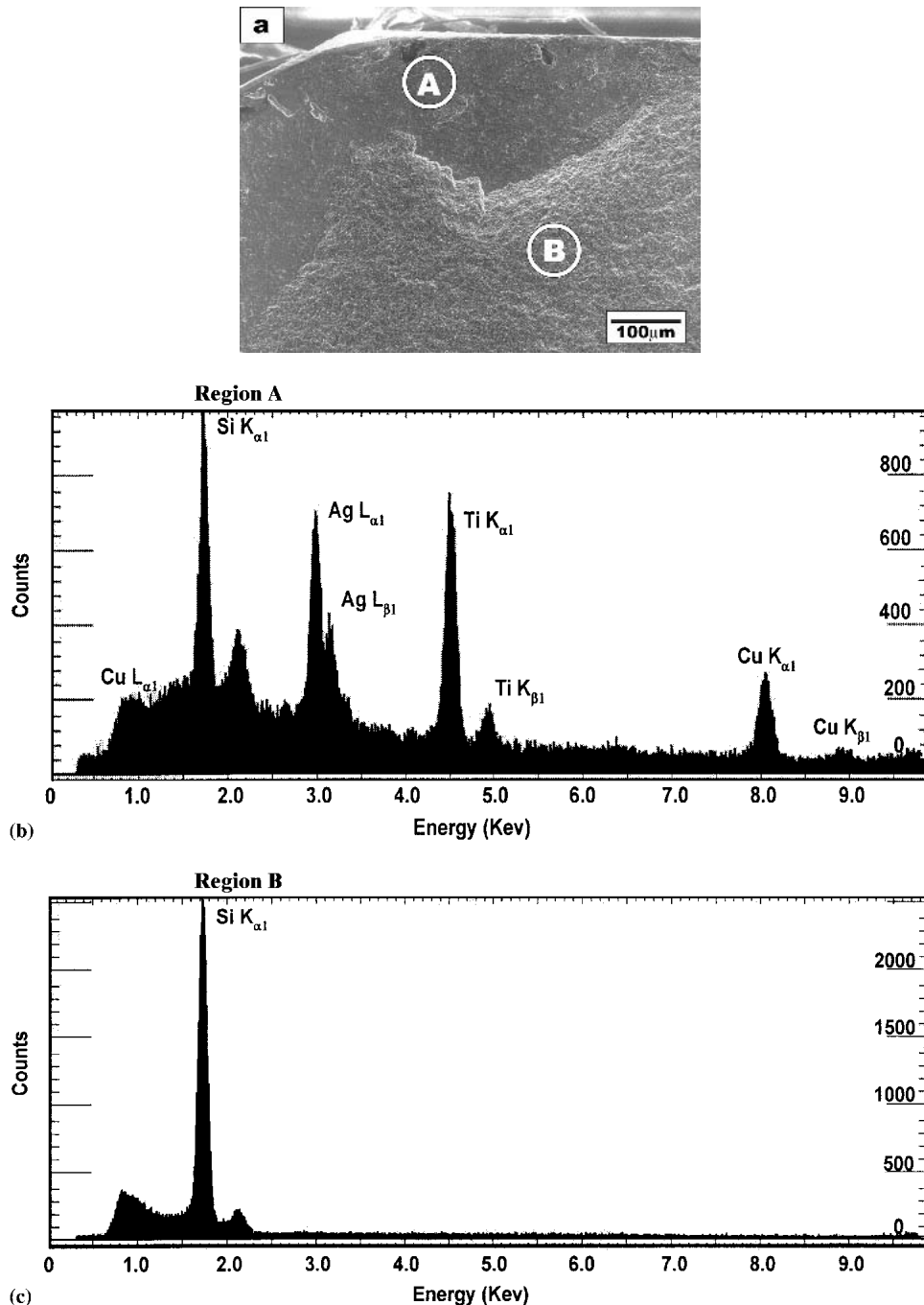


Fig. 5 The fracture surface of  $\text{Si}_3\text{N}_4/\text{Cu}$  0.2 mm/S.S. 316 joint (a) SEM; (b) EDS for region-A; (c) EDS for region-B

ing alloy needs to be considered for the proper calculation of the residual stress developed within the joint. The inverse variations of the maximum residual stress and the measured fracture strength indicate that the microstructural effects near the joint interface should not be overlooked in the residual stress computation for brazed Si<sub>3</sub>N<sub>4</sub>/stainless steel joints with a Cu-interlayer where appreciable microstructure changes take place during brazing. Therefore, the consideration of the microstructural change is required to assess the validity of the FEA for residual stress. Indeed, consistent data between the maximum tensile residual stress and fracture strength data for the joint depending on the Cu-interlayer of variable thickness can only be obtained by taking the microstructural change into account.

Figure 4 shows variations in fracture shape and initiation site depending on the thickness of the inserted Cu-interlayer. The use of a 0.1 mm thick Cu-interlayer showed fractured shapes resembling concave round domes on the ceramic side. The concave dome on the ceramic side is reported to be an indication of the presence of substantial tensile residual stress.<sup>[5]</sup> The fracture was observed to occur for the joint using a 0.1 mm Cu-interlayer slightly away from the Si<sub>3</sub>N<sub>4</sub>/brazing alloy joint interface as shown in Fig. 2. The experimental observation seemed to be consistent with the FEA calculation regarding the location for the maximum residual stress. Similar fractured shapes were reported for Si<sub>3</sub>N<sub>4</sub>/S45C steel<sup>[19]</sup> or Si<sub>3</sub>N<sub>4</sub>/Inconel joints.<sup>[20]</sup>

However, the fracture for the Si<sub>3</sub>N<sub>4</sub>/Cu 0.2 mm/stainless steel joint initiated at the Si<sub>3</sub>N<sub>4</sub>/brazing alloy interface, and appeared to propagate rather flat and almost parallel to the joint interface. The crack extended toward the inner volume of Si<sub>3</sub>N<sub>4</sub> as shown in Fig. 4(b). For the Si<sub>3</sub>N<sub>4</sub>/Cu 0.4 mm/stainless steel joint, the crack, which initially paralleled the interface, was deflected from the interface shaping concave dome with a less salient dome-like angle when compared with that for the Si<sub>3</sub>N<sub>4</sub>/Cu 0.1 mm/joint. Then, the compressive flexural loading is considered to be responsible for the final deflection away from the interface. The increase of residual stress for the joint compared with that for the joint with a 0.1 mm thick Cu-interlayer, together with the reduction of the fracture strength, is shown in Fig. 3. The crack path in the thermo-mechanically loaded ceramic/metal (Si<sub>3</sub>N<sub>4</sub>/Cu/S45C) joint was investigated numerically. It was concluded that the reduction in the crack-deflected angle from the interface, which determines a dome-like angle in this case, could be an indication of reduced residual stress within the joint.<sup>[21]</sup>

Figure 5 shows the detailed microstructure and EDS analysis of the fractured face on the Si<sub>3</sub>N<sub>4</sub> side for the Si<sub>3</sub>N<sub>4</sub>/Cu 0.2 mm/stainless steel joint. It appears that the fracture initiated at region-A (at the immediate interface between Si<sub>3</sub>N<sub>4</sub> and brazing alloy) and propagated toward the region-B (Si<sub>3</sub>N<sub>4</sub>). EDS evaluation revealed that region-A contains a reaction product, as opposed to region-B which contains pure silicon nitride. The EDS evaluations seemed to be consistent with the findings, which the fracture initiated at the immediate joint interface (Fig. 2 and 4).

## 4. Conclusion

The entire dissolution of the 0.1 mm thick Cu-interlayer into the Cusil ABA brazing alloy changes the microstructure of the joint interface. The finite element analysis of residual stress, in

which changes in the microstructure of the joint interface were measured, directly reflected the inverse variation in the measured fracture strength as a function of the Cu-interlayer's thickness. These results demonstrate that microstructural change in the neighborhood of the interface for the brazed Si<sub>3</sub>N<sub>4</sub>/stainless steel joint with the Cu-interlayer should be included in the FEA procedure to estimate residual stress. A qualitative agreement between the experimental findings, including fracture initiating site and the inverse variation of residual stress, were obtained.

## Acknowledgment

This study was supported by The Korean Science and Education Foundation (1999-2-301- 014-3).

## References

1. M. Savitz: "Commercialization of Advanced Structural Ceramics," *Am. Ceram. Soc. Bull.*, 1999, 78(3), pp. 52-56.
2. A.V. Durov, B.D. Kostjuk, A.V. Shevchenko, and Y.V. Naidich: "Joining of Zirconia to Metal With Cu-Ga-Ti and Cu-Sn-Pb-Ti Fillers," *Mater. Sci. Eng.*, 2000, 290, pp. 186-89.
3. M.R. Rijnders and S.D. Peteves: "Joining of Alumina Using a V-Active Filler Metal," *Scripta Materialia*, 1999, 41(10), pp. 1137-46.
4. S.P. Kovalev, P. Miranzo, and M.I. Osendi: "Finite Element Simulation of Thermal Residual Stresses in Joining Ceramics With Thin Metal Interlayers," *J. Am. Ceram. Soc.*, 1998, 81(9), pp. 2342-48.
5. D. Munz, M.A. Sckuhr, and Y. Yang: "Thermal Stresses in Ceramic-Metal Joints With an Interlayer," *J. Am. Ceram. Soc.*, 1995, 78(2), pp. 285-90.
6. S. Kang and H.J. Kim: "Design of High-Temperature Brazing Alloys for Ceramic-Metal Joints," *Welding Research*, 1995, Suppl., pp. 289S-95S.
7. S.D. Peteves, G. Ceccone, M. Paulasto, V. Stamos, and P. Yvon: "Joining Silicon Nitride to Itself and to Metals," *J. Metals*, 1996, p. 48-77.
8. D. Sciti, A. Bellosi, and L. Esposito: "Bonding of Zirconia to Super Alloy With the Active Brazing Technique," *J. Eur. Ceram. Soc.*, 2001, 21, pp. 45-52.
9. A. Guedes, A.M.P. Pinto, M. Vieira, and F. Viana: "Multilayered Interface in Ti-Macor Machinable Glass-Ceramic Joints," *Mater. Sci. Eng.*, 2001, A301, pp. 118-24.
10. R.K. Shiu, S.K. Wu, J.M. O, and J.Y. Wang: "Microstructural Evolution at the Bonding Interface During the Early-Stage Infrared Active Brazing of Alumina," *Metall. and Material. Transac. A.*, 2000, pp. 2527-36.
11. P. Yang, B.N. Turman, S.J. Glass, J.A. Halbleib, T.E. Voth, F.P. Gerstle, B. Mckenzie, and J.R. Clifford: "Braze Microstructure Evolution and Mechanical Properties of Electron Beam Joined Ceramics," *Mater. Chem. Phys.*, 2000, 64, pp. 137-46.
12. K.N. Lee: "Current Status of Environmental Barrier Coatings for Si-Based Ceramics," *Surf. Coatings Tech.*, 2000, pp. 1-7.
13. S. Ahat, H. Weidong, S. Mei, and L. Le: "Joint Shape, Microstructure, and Shear Strength of Lead-Free Solder Joints With Different Component Terminations," *J. Electron. Mater.*, 2002, 31(2), pp. 136-41.
14. J. Mei and P. Xiao: "Joining Metals to Zirconia for High Temperature Applications," *Scripta Materialia*, 1999, 40(5), pp. 587-94.
15. *ABAQUS/Standard User's Manual*, Hibbit, Kaarlson & Sorenson Inc, USA, 2001.
16. D. Huh and D. Kim: "Joining of AlN to Cu Using In-Base Active Brazing Fillers," *J. Mater. Res.*, 1997, 13(4), pp. 1048-55.
17. H. Hao, Y. Wang, Z. Jin, and X. Wang: "Joining of Zirconia Ceramic to Stainless Steel and to Itself Using Ag<sub>55</sub>Cu<sub>38</sub>Ti<sub>5</sub> Filler Metal," *J. Am. Ceram. Soc.*, 1995, 78(8), pp. 2157-60.
18. S. Tanaka: "Residual Stress Relaxation in Si<sub>3</sub>N<sub>4</sub>-Metal Joined Systems," *MRS Int. Mtg. Adv. Mater.*, 1988, 8, pp. 125-30.
19. H. Kobayashi, Y. Arai, H. Nakamura, and T. Sato: "Strength Evaluation of Ceramic-Metal Joints," *Mater. Sci. Eng.*, 1991, A143, pp. 91-102.
20. J.-W. Park, P.F. Mendez, and T.W. Eagar: "Strain Energy Distribution in Ceramic-to-Metal Joints," *Acta Metall.*, 2002, 50, pp. 883-99.
21. J.H. Kim and S.B. Lee: "Stress Intensity Factors and Crack Initiation Directions for Ceramic-Metal Joint," *Theor. Appl. Fracture Mech.*, 1998, 30, pp. 27-38.